Published in final edited form as:
J Neurochem. 2008 July ; 106(2): 860–874. doi:10.1111/j.1471-4159.2008.05459.x.

Adaptation to chronic MG132 reduces oxidative toxicity by a CuZnSOD-dependent mechanism

Rehana K. Leak[1,*], **Michael J. Zigmond**[1,2,3], and **Anthony K. F. Liou**[1]

[1] Department of Neurology, Pittsburgh Institute of Neurodegenerative Diseases, University of Pittsburgh, Pittsburgh, PA 15260 USA

[2] Department of Neurobiology, Pittsburgh Institute of Neurodegenerative Diseases, University of Pittsburgh, Pittsburgh, PA 15260 USA

[3] Department of Psychiatry, Pittsburgh Institute of Neurodegenerative Diseases, University of Pittsburgh, Pittsburgh, PA 15260 USA

Abstract

To study whether and how cells adapt to chronic cellular stress, we exposed PC12 cells to the proteasome inhibitor MG132 (0.1 μM) for 2 weeks and longer. This treatment reduced chymotrypsin-like proteasome activity by 47% and was associated with protection against both 6-hydroxydopamine (6-OHDA, 100 μM) and higher dose MG132 (40 μM). Protection developed slowly over the course of the first 2 weeks of exposure and was chronic thereafter. There was no change in total glutathione levels after MG132. Buthionine sulfoximine (100 μM) reduced glutathione levels by 60%, but exacerbated 6-OHDA toxicity to the same extent in both MG132-treated and control cells and failed to reduce MG132-induced protection. Chronic MG132 resulted in elevated antioxidant proteins CuZn superoxide dismutase (SOD, +55%), MnSOD (+21%), and catalase (+15%), as well as chaperone heat shock protein 70 (+42%). Examination of SOD enzyme activity revealed higher levels of CuZnSOD (+40%), with no change in MnSOD. We further assessed the mechanism of protection by reducing CuZnSOD levels with two independent siRNA sequences, both of which successfully attenuated protection against 6-OHDA. Previous reports suggested that artificial overexpression of CuZnSOD in dopaminergic cells is protective. Our data complement such observations, revealing that dopaminergic cells are also able to use endogenous CuZnSOD in self-defensive adaptations to chronic stress, and that they can even do so in the face of extensive glutathione loss.

Keywords

6-hydroxydopamine; dopamine transporter; glutathione; Parkinson’s disease; proteasome

Introduction

Neurodegenerative conditions such as sporadic Parkinson’s disease (PD) occur only in a minority of individuals and usually do not manifest themselves until advanced age. One explanation for this phenomenon is that cells possess self-defenses against cellular stress, but that these adaptive mechanisms become less effective with age and in certain disease states. A type of cellular stress thought to be present for decades in individuals with PD is the presence of misfolded and damaged proteins, resulting in the progressive accumulation of dystrophic

[*]Please address correspondence to: Rehana Khan Leak, Ph.D., 7026 Biomedical Science Tower 3, Pittsburgh Institute for Neurodegenerative Diseases, University of Pittsburgh, Pittsburgh, PA, 15260, Tel: (412) 383-9051, FAX: (412) 624-7327, leakrk@upmc.edu.

neurites and inclusions across many brain regions (Braak et al. 2003). This observation raises the possibility that in PD affected cells deal with a high burden of damaged proteins over an extended timeframe. Studying adaptive defenses to such cellular stressors may yield insight into what keeps illnesses at bay in most individuals and/or what delays neurodegeneration in individuals who do finally develop disease. Moreover, learning how to boost such endogenous defenses pharmacologically without applying stress *per se* may lead to treatments that slow the progression of neurodegeneration even further.

The proteasome is a multicatalytic complex engaging in proteolysis of misfolded, oxidized, and aggregated proteins. A reduction in its activity has been observed in Alzheimer's disease, PD, and with advancing age (Conconi et al. 1996; Friguet et al. 2000; Keller et al. 2000a; Keller et al. 2000b; Lopez Salon et al. 2000; Merker et al. 2001; Keck et al. 2003; McNaught et al. 2003). For example, there is an average 44% loss in chymotrypsin-like proteasome activity in postmortem PD nigra (McNaught et al. 2003). If and how dopaminergic cells might adapt to this burden to prolong the course of degeneration in PD has not been explored, but deserves further study, both in the human disease as a function of illness duration and in those PD models using pharmacological proteasome inhibitors (Rideout *et al.* 2001; McNaught *et al.* 2002; Ding *et al.* 2003; Fornai *et al.* 2003; Mytilineou *et al.* 2004; Inden *et al.* 2005; Miwa *et al.* 2005; Rideout *et al.* 2005; Sun *et al.* 2006). Many such reports have indicated that short-term proteasome inhibition with pharmacological compounds can indeed elicit protection against cellular stress (Bush et al. 1997; Lee and Goldberg 1998b; Lee et al. 2004; Sawada et al. 2004; Inden et al. 2005; Yamamoto et al. 2007). Furthermore, proteasome inhibition has been shown to activate both pro-survival and pro-apoptotic pathways, with the former response predominating at low concentrations of the inhibitor (Lin et al. 1998; Yew et al. 2005). Therefore, it seemed possible that even chronic exposure to a proteasome inhibitor at a subtoxic concentration might elicit an adaptive response that could be dissected *in vitro*. In support of our hypothesis, Ding and colleagues noted that dopaminergic SH-SY5Y cells were rendered more resilient against oxidative stress and serum withdrawal with 12 or more weeks of exposure to a proteasome inhibitor, by an unknown mechanism (Ding et al. 2003). Such defensive responses to stress are akin to the phenomenon of "preconditioning" or "tolerance" in studies of ischemia, where it has long been known that sublethal acute ischemic episodes protect against longer ischemic episodes (Murry et al. 1986; Kitagawa et al. 1990). Studies of preconditioning, however, have been limited to short-term exposures to sublethal stressors. The present report extends those studies to a model with a longer-term stress in order to better emulate the chronic conditions in human neurodegenerative diseases and aging.

One of the best characterized proteasome inhibitors is MG132, a potent inhibitor of the chymotrypsin-like activity of the proteasome that also affects cathepsins and calpains, effectively increasing the burden of misfolded proteins and concomitant cellular stress (Lee and Goldberg 1998a; Kisselev and Goldberg 2001; Fuertes et al. 2003; Rodgers and Dean 2003). Thus, in the present study, MG132 was applied to PC12 cells from days to weeks, and then for months onwards, to examine whether this chronic stress would alter the vulnerability of these dopaminergic cells to further injury. Here we report the novel observation that a chronic treatment to raise damaged protein levels actually resulted in higher resilience against oxidative stress, that the adaptive response was mediated at least in part by CuZnSOD, and that protection was uncoupled from extensive glutathione (GSH) loss.

Materials and Methods

Chemicals and Antibodies

All chemicals were purchased from Sigma-Aldrich (St. Louis, MO), unless specified otherwise. Primary and secondary antibodies were purchased and used as follows: mouse anti-tyrosine hydroxylase (TH; 1:1000 for immunocytochemistry, 1:10,000 for immunoblotting, Chemicon,

Temecula, CA), rabbit anti-MnSOD (1:5000, Upstate Inc, Charlottesville, VA), rabbit anti-CuZnSOD (1:500, Upstate Inc), mouse anti-catalase (1:5000, Sigma), rabbit anti-inducible heat shock protein 70 (Hsp 70; 1:1000, Stressgen, San Diego, CA), mouse anti-ubiquitin conjugated proteins (1:500, Santa Cruz Biotechnology, Santa Cruz, CA), mouse anti-α-tubulin (1:5000, Sigma), mouse anti-β-actin (1:50,000, Sigma), rabbit anti-β-actin (1:10,000, Abcam, Cambridge, MA), rabbit anti-GSH (1:300, Chemicon), infrared anti-rabbit and anti-mouse IgG (1:10,000 for Western blots, 1:1000 for In Cell Westerns, LI-COR Biotechnology, Lincoln, NA), and Alexa Fluor 488 goat anti-mouse IgG (1:1000, Molecular Probes, Eugene, OR). Omission of either primary or secondary antibodies from the assays resulted in loss of signal.

Cell maintenance

PC12 cells were left in their undifferentiated state so as to be able to continuously apply MG132 out to a maximum of 6 months as the studies proceeded. In preliminary studies, however, we found a lack of high-affinity tritiated dopamine (^{3}H-DA) uptake in undifferentiated PC12 cells. Thus, to ensure rapid uptake of 6-OHDA and specific oxidative breakdown within the intracellular milieu, we obtained PC12 cells stably transfected with the human dopamine (DA) transporter under control of the CMV promoter (gift of Gonzalo E. Torres, University of Pittsburgh). These cells were maintained at 37°C with 5% CO_2 in low glucose DMEM (InVitrogen, Carlsbad, CA), supplemented with 5% horse serum, 5% fetal bovine serum (InVitrogen), and 50 μg/ml G418 (Cellgro, Herndon, VA). Cells were plated at a density of 1061 cells per mm^2 (30,000/well in a 96-well plate) on collagen-coated plates (Becton Dickinson, Franklin Lakes, NJ). Treatments or assays were typically made or initiated 24 hr after plating. For siRNA treatments only, cell density was increased to 1415 cells per mm^2 (40,000/well in a 96-well plate) to achieve high confluence at the time of transfection.

Toxin treatments

To produce chronic stress, cells were maintained in 0.1 μM peptide aldehyde MG132 (Cbz-leu-leu-leucinal), purchased from EMD Bioscience (San Diego, CA). MG132 was made up as a 1 mM stock solution in dimethyl sulfoxide (DMSO) and then freshly diluted only 1 μl per 10 ml media to minimize DMSO exposure. For the second, challenge treatments we chose 6-OHDA (Sigma-Aldrich Co. or Regis Technologies, Inc., Morton Grove, IL) and high dose MG132. Although many *in vitro* studies of 6-OHDA use long incubation intervals, 6-OHDA oxidizes rapidly to hydrogen peroxide and other toxic by-products under typical culturing conditions (Ding et al. 2004; Hanrott et al. 2006; Saito et al. 2007). Thus, we prepared 6-OHDA in a vehicle composed of 0.15% ascorbic acid and 10 mM of the metal chelator diethylenetriamine pentaacetic acid (DETAPAC), flushed with nitrogen for 10 min before use to help remove oxygen. 6-OHDA made in this vehicle was then diluted 10-fold in media added to the wells for 30 min. This procedure was designed to limit the potential confound of oxidation products within the media and increase intracellular breakdown (Clement et al. 2002; Ding et al. 2004). MG132 was left in the media during and after 6-OHDA, because we reasoned that cells in neurodegenerative conditions in aged humans would continue to suffer from cellular stress and misfolded proteins while exposed to an oxidative insult. For a challenging, test dose of MG132, 40 μM was chosen from a pilot dose-response curve, and, unlike 6-OHDA, MG132 or the same volume of DMSO were left in for another 24 hr before cellular viability was assessed as described below.

Studies of chronic MG132-induced changes in vulnerability to 6-OHDA were initiated with exposure to the inhibitor ranging from 2 weeks to 6 months and averaged across time. Comparisons were always made to control, non-MG132 treated cultures maintained and assayed side-by-side with simultaneous passaging or plating at the same density. No difference in results were observed with exposure to MG132 beyond that of 2 weeks; however, slight shifts in the EC50 for toxins and in the degree of MG132-induced protection were observed

across toxin batches and/or periods of storage of these compounds. This was especially true for 6-OHDA, as reported by us previously (Ding et al. 2004; Lin et al. 2008). Therefore, small aliquots of both toxins were rapidly flash-frozen as concentrated stocks, which helped minimize inter-experimental variability for statistical analyses.

To produce GSH depletion, buthionine sulfoximine (BSO, 100 μM) was freshly dissolved in sterile phosphate buffered saline (PBS) as a 10 mM stock. Twenty-four hr after plating, cells were treated in media with indicated concentrations of BSO, or the same volume of PBS, for 24 hr before 6-OHDA. BSO was then left in during and after 30 min 6-OHDA treatments until the indicated time of assay. Details on ensuring BSO efficacy follow, in the section below on In Cell Western infrared assays for GSH.

Tyrosine hydroxylase (TH) immunocytochemistry

For staining cells with antibodies against TH, a rate limiting enzyme for DA biosynthesis, cells were fixed with 2% paraformaldehyde in PBS. Non-specific secondary binding was then minimized by blocking in 10% normal goat sera (Jackson Immunochemicals, West Grove, PA) diluted in 0.3% triton-X 100 in PBS for 1 hr. Cells were subsequently incubated overnight with a mouse antibody against TH diluted in 1% normal serum and 0.3% triton-X in PBS. Cells were then washed three times in PBS and subjected to secondary incubation with Alexa Fluor 488 goat anti-mouse IgG diluted in 2% normal serum and 0.3% triton-X in PBS. At the end of 1 hr cells were washed again 2 times in PBS and stained with a 10 μg/ml solution of Hoechst 33258 (bisbenzimide) for 20 min before a final wash. Photography under brightfield, UV, or FITC illumination was then performed on a Nikon Inverted Eclipse TE 2000 microscope (Fryer Inc. Carnegie, PA).

Western Blotting

Cells were lysed for immunoblotting with Cell Lysis Buffer (Cell Signaling, Danvers, MA) with added protease inhibitor cocktail (Sigma-Aldrich). Lysates were sonicated for 5 sec and subjected to centrifugation (15 min at 15,000 g) for measurements of protein content in the supernatant by the bicinchoninic acid (BCA) method (Pierce, Rockford IL). Equal amounts of protein (20 μg) from each treatment were separated on SDS gels and transferred to Immobilon FL PVDF membranes (BioRad Laboratories, Hercules, CA). Non-specific binding was reduced by incubating membranes in a fish serum blocking solution at full strength (LI-COR Biotechnology) for 1 hr prior to overnight treatment at 4°C with primary antibodies diluted in the same blocking solution. Mouse or rabbit anti-β-actin antibodies were always used as a concurrent loading control. Blots were then washed 3 times in Tris-buffered saline (TBS) with 0.1% Tween (Biorad) and incubated 1 hour with infrared secondary antibodies raised against the appropriate species, fluorescing at either 700 or 800 nm. After 3 washes in TBS-tween, blots were visualized on an Odyssey Infrared Imager (LI-COR Biotechnology) and fluorescent signal from each protein band quantified with Odyssey software.

Proteasome activity assay

Chymotrypsin-like proteasome activity of the cytosolic 26S particle was assessed using published methods, where emitted fluorescence is in direct proportion to proteasome activity (Kisselev and Goldberg 2005). Briefly, we suspended cells in 50 mM Tris-HCl, pH 7.5, 250 mM sucrose, 5 mM $MgCl_2$, 2 mM ATP, 1 mM DTT, 0.5 mM EDTA, and 0.025% digitonin. Following 5 min of permeabilization, cytosol was separated out by centrifugation at 20,000 g for 15 min at 4°C. Cytosolic extract was then added to the assay buffer at a final dilution of 0.25 μg/μl, as determined by the BCA method. The buffer consisted of 50 mM Tris-HCl, pH 7.5, 40 mM KCl, 5 mM $MgCl_2$, 0.5 mM ATP, 1 mM DTT, and 0.05 mg/ml BSA. Fluorogenic substrate for the 20S proteasome, Suc-LLVY-amc (BIOMOL International, Plymouth Meeting, PA) was freshly prepared and then added to the assay buffer at 100 μM to specifically

measure cleavage at the chymotrypsin-like site. For each group, duplicate samples were always pretreated for 30 min at 37°C with 20 μM epoxomicin (Peptides International, Louisville, KY). Epoxomicin is considered a more specific inhibitor of all three proteasome sites and was used to estimate the fraction of proteolytic activity resulting from enzymes other than the proteasome during the assay (Kisselev and Goldberg 2005). Fluorescence was recorded every 20 min over the course of one hour (excitation 380 nm, emission 460 nm), and the raw values at each timepoint compared to the linear range of 7-amino-4-methylcoumarin standards (AMC, Bachem, Torrance, CA), diluted 0.1–10 μM.

Viability assays

Cell viability was measured 24 hr after treatment in two ways, by measuring ATP levels or counting viable nuclei. First, ATP levels were assayed by a proprietary luciferase based reaction with Cell Titer Glo (Promega Inc, Madison, WI), added according to the manufacturer's instructions and read 20 min later on a microplate reader (L-Max II, Molecular Devices, Sunnyvale, CA). Second, cells were fixed with a 2% paraformaldehyde solution in PBS and stained with Hoechst solution as above. Blind counts of viable cells were performed following UV-illuminated digital capture of nuclei from the center of each well, as described previously (Leak et al. 2006). For one set of experiments, ATP level assays were also performed 48 hr after 6-OHDA removal instead of 24 hr, as indicated in the Results section.

^{3}H-DA uptake

Cells were incubated with 200 nM ^{3}H-DA (specific activity 59.3 Ci/mmol, American Radiolabeled Chemicals, St. Louis, MO) in PBS for 15 min at 37°C (Leak et al. 2006). Negative control wells were incubated with the high-affinity DA transporter blocker nomifensine (40 μM) for 10 min prior to and during the assay. Cells were then washed 3 times with PBS and total tritium extracted with ethanol and perchloric acid for counts by liquid scintillation spectroscopy (Beckman LS-1800; Beckman Coulter, Inc.; Fullerton, CA). Counting efficiency for tritium was 0.58, and results were expressed as DPM.

Glutathione assay

For measuring total GSH in a relatively high-throughput manner, an assay was developed using the infrared In Cell Western system (LI-COR Biotechnology). A rabbit antibody raised against both oxidized and reduced GSH was applied together with a mouse antibody against α-tubulin and visualized with infrared secondary IgGs. Specificity controls for the GSH antibody included various concentrations of BSO treatments to ensure dose-dependent loss of GSH staining, as well as depletion of signal by preadsorption of the antibody with excess GSH tripeptide purchased in its reduced form (Sigma-Aldrich). A 100 μM concentration of BSO was then chosen for viability experiments, as it did not by itself result in any loss of α-tubulin signal or of ATP levels by Cell Titer Glo, and so was deemed non-toxic. For the remaining GSH assays, cells were fixed with paraformaldehyde at 3, 6, or 24 hr after treatment with BSO ± 6-OHDA and stored in PBS-azide until incubation in 10% normal goat serum in 0.3% triton-X 100 in PBS for 1 hour. Then cells were then exposed overnight to rabbit anti-GSH and mouse anti-α-tubulin diluted in 1% normal goat serum and 0.3% triton-X in PBS. The following day, cells were rinsed 3 times in PBS and incubated for 1 hour in infrared goat anti-mouse (700 nm) and goat anti-rabbit (800 nm) secondary IgG, diluted in 2% normal serum and 0.3% triton-X in PBS. Plates were finally washed 3 times in PBS and infrared emissions from each well-bottom read on the Odyssey Imager. GSH levels as measured by this system were expressed as anti-GSH fluorescence intensity divided by anti-α-tubulin fluorescence intensity. The original images generated by this sensitive system are in a gray scale rather than color (as shown in Figures) and their bit-depth of 16 yields 2^{16} or 65,536 intensity levels.

SOD activity assays

Cells were harvested in PBS 24 hr after plating. An aliquot of this was removed for BCA protein content assay as usual. Cells in PBS were spun at 2,000 g for 10 min at 4°C and resuspended and homogenized in 20 mM HEPES buffer, pH 7.2, containing 1 mM EGTA, 210 mM mannitol, and 70 mM sucrose. The homogenized solution was recentrifuged at 1500 g for 5 min at 4°C, the supernatant collected, and 5 μg protein from each sample mixed with tetrazolium salt in each well as per manufacturer's directions for detection of superoxide radicals (Cat No.706002; Cayman Chemicals, Ann Arbor, MI). A second set of duplicate samples were simultaneously treated with 2 mM potassium cyanide, an inhibitor of CuZnSOD, to permit assessment of MnSOD activity (Saggu et al. 1989). Absorbance was read at 450 nm and enzyme activity calculated from absorbance of SOD standards, after ensuring raw values were within their linear range.

RNA interference

For RNA interference, cells were plated at high confluency in accordance with the manufacturer's instructions for Lipofectamine 2000 (Invitrogen). siRNA concentrations were based on the manufacters's recommendations for rat cell lines (500 pmoles for 6-well plates with 3.5 cm diameter wells). Our pilot testing range for knockdown by immunoblotting was 25–500 pmoles for each siRNA sequence. We chose to focus upon concentrations that produced a knockdown of CuZnSOD back to naïve control values within 24 hr, so as to minimize adverse effects upon basal viability by long-term loss of a critical protein. From the pilot data, we chose to treat cells with 300 pmoles "All Stars" negative control siRNA (Qiagen Inc, Valencia, CA) or CuZnSOD siRNA (see below) in Opti-MEM/Glutamax transfection media (Invitrogen) with 5 μl Lipofectamine per 100 pmoles siRNA in 6-well plates (31 pmoles/cm^2). The proprietary, negative control siRNA was designed to have no known homology to mammalian genes but enter the RNA-Induced Silencing Complex (RISC). Two different CuZnSOD sequences were used, one from Qiagen (antisense sequence rUUA AUC CUG UAA UCU GUC CdTdG) and one from Dharmacon (Lafayette, CO; antisense sequence 5′-P.UUC ACC GCU UGC CUU CUG CUU). Both sequences gave similar knockdown values at 300 pmoles.

For viability experiments in 96-well format (0.6 cm diameter wells), cells plated at the same number per unit surface-area were treated with 8.82 pmoles negative control or CuZnSOD siRNA (31 pmoles/cm^2, final concentration of 88 nM). After 5 hr, Opti-MEM was replaced with regular medium and cells were treated 24 hr later with 6-OHDA or vehicle as usual, except that the concentration of 6-OHDA was doubled (200 μM) since the cell plating density for transfections was higher than before and affected the EC50. Cells were assayed with Cell Titer Glo 24 hr after 6-OHDA as usual.

Statistical analyses

Data are presented as means ± SEM from 3–7 independent experiments, each performed in triplicate wells or more and analyzed using two-tailed t-tests when there were only 2 groups or otherwise by ANOVA (SPSS V10.1, SPSS Inc., Chicago, IL). Post-hoc comparisons following ANOVA were performed using the method of Bonferroni. Results were deemed significant when $p \leq 0.05$.

Results

MG132 caused no overt change in morphological appearance of PC12 cells

MG132 treated cells showed no detectable change in cellular appearance or tyrosine hydroxylase (TH) enzyme expression, as assessed with brightfield images (Figure 1A, B), Hoechst nuclear staining (Figure 1C, D), and immunocytochemistry (Figure 1E, F).

Immunoblotting with anti-TH antibodies also revealed no MG132-induced change in TH protein levels (Figure 1G), in support of the immunocytochemical results. Further, no neurite extension or signs of differentiation were observed over the course of 6 months of exposure.

MG132 decreased proteasome activity

In our model, chronic exposure to 0.1 μM MG132 reduced chymotrypsin-like activity in cytosolic extracts by 47% (Figure 2A), indicating that our toxin was effective at this concentration. Fluorescence increased linearly over time during the assay for proteasome activity, but with no further change between groups (20 min reading shown in Figure 2A). As a negative control, treatment of aliquots of the same extracts with epoxomicin (20 μM) before and during the assay itself dropped fluorescent emissions in both control and MG132 samples by an average of 99%.

With successful reduction of proteasome activity, one would expect substrate turnover to decrease and the levels of ubiquitin-conjugated proteins to rise. Thus, we probed control and MG132 treated cells for ubiquitin-conjugated proteins. In MG132 treated cells we found a trend for increased levels of such proteins by two-tailed t-test ($p = 0.076$, one-tailed t-test p value = 0.038, 6 independent sets; Figure 2B). The 42% rise in ubiquitin conjugates with proteasome inhibition was noted by quantifying the *entire* visible MW range (250 to 15 kDa), but the typical spread of proteins most affected were those at higher molecular weights. This pattern has been noted in figures from other authors, some of them also using MG132 (Fujimuro et al. 1994; Elkon et al. 2001; Ohtake et al. 2007). We show a representative immunoblot from two sets of experimental samples harvested 6 months apart, to illustrate how the response did not appear to vary over time (Figure 2B, right panel).

MG132 protected against oxidative stress and higher concentrations of MG132

Chronic MG132 exposure attenuated the toxic effects of 6-OHDA as well as a high concentration of MG132, as measured by both ATP level assay (Cell Titer Glo) and the Hoechst nuclear stain (Figure 3A–D). The MG132-induced rise in viability following 6-OHDA treatment typically ranged from 25–30% with these assays (Figure 3A, B). A similar pattern was observed for high dose MG132 post-treatment, with an approximately 30% rise in viability apparent with both assays (Figure 3C, D). Subsequent experiments focused solely upon 6-OHDA, as it is considered to be a classic model of oxidative stress for catecholaminergic cells (Zigmond and Keefe 1997). Furthermore, as ATP levels are likely to be more indicative of functionally protected cells than the appearance of Hoechst-stained intact nuclei, the Cell Titer Glo assay was chosen for subsequent viability assays.

The PC12 cells used here were stably transfected with the human DA transporter to achieve rapid, high-affinity transport of 6-OHDA within a short interval and prevent its extracellular breakdown in media (see Methods; discussed at length by Clement and colleagues (Clement et al. 2002)). In order to gauge whether MG132 by itself might reduce intracellular entry of 6-OHDA, we examined the uptake of ^{3}H-DA across the plasma membrane. We found that chronic MG132 treatment did not reduce ^{3}H-DA uptake, instead, a 36% increase was observed (Figure 3E). In contrast, the DA transport blocker nomifensine applied during the assay effectively reduced ^{3}H-DA uptake, supporting the specificity of our measure. We inferred from these data that any MG132-induced protection against 6-OHDA could not be attributed to reductions in toxin entry.

Protection against 6-OHDA was not elicited or sub-maximal with short-term MG132 treatment, and was lost upon MG132 removal

In order to examine whether protection could be elicited with a short interval of exposure to MG132, naïve PC12 cells were exposed to 0.1 μM MG132 for 24 hr prior to 6-OHDA

treatment. MG132 was then left in during and after 6-OHDA (24 hr), as this was also the protocol for all the chronic stress experiments (see Methods). Thus, the previously naïve cells had experienced a total interval of 48.5 hr of 0.1 μM MG132 at the time of viability assay (Figure 4A). Such short-term treatment failed to confer any protection, cause significant cell loss, or hyperproliferation by itself, suggesting that a longer period of exposure was required for protection and supporting the hypothesis that growth rates remained constant. Then we examined closely the interval between lack of protection (1 day exposure before application of 6-OHDA) and the ≥14 day period. For this, naïve control cells were treated with 0.1 μM MG132 for 4, 8, or ≥14 days at time of 6-OHDA. Thus, the 4 and 8 day groups were plated at day 3 and day 7 for 6-OHDA treatment the next day, and assayed at day 5 and 9, one day after 6-OHDA, respectively. In these experiments, we found a smaller degree of protection at 4 days (20% rise in viability from controls) and 8 days (14% rise) relative to exposure for 14 days or longer (32% rise; Figure 4B).

We then proceeded to characterize basal viability in cells grown for 0, 3, 7, or >14 days in MG132, and plated for Cell Titer Glo assay after an additional 24 hr (0, 4, 8, or >14 days at assay) or 48 hr (0, 5, 9, or >14 days when assayed). No differences in cell density were observed across time between any groups (Figure 4C). Next, we asked whether the MG132 treatment simply delayed cell death for 24 hrs or could effect longer-lasting protection (48 hr after removal of 6-OHDA). We found robust MG132-induced protection even 2 days after 6-OHDA removal (Figure 4D). Finally, we examined if the protection would linger in the long-term absence of MG132. However, we found that a removal of the stimulus for 2 weeks resulted in loss of protection and a complete reversal back to the original state of vulnerability to 6-OHDA (Figure 4E).

MG132-induced protection against 6-OHDA was not mediated by an increase in GSH

Previous studies suggested that short-term treatment with proteasome inhibitors increased GSH synthesis in PC12 cells and may have conferred protection against 6-OHDA and hydrogen peroxide (Yamamoto et al. 2007). We therefore investigated whether long-term treatment with MG132 protected PC12 cells against 6-OHDA by a GSH-dependent mechanism. To accomplish this, we first developed the assay for total GSH described in the Methods section and illustrated in Figure 5A, B. An immunocytochemical method such as this will not discriminate free GSH from GSH-protein adducts, but one would expect both measures to rise and fall in parallel under most circumstances. First we verified in naïve controls that BSO treatment for 24 hr reduced the GSH signal in a concentration-dependent manner without affecting cell density (12.5 to 100 μM). Higher concentrations of BSO resulted in loss of α-tubulin signal (data not shown), thus, we chose the 100 μM concentration for our following experiments.

Naïve and MG132 treated cells were then exposed to BSO ± 6-OHDA or their respective vehicles to examine whether GSH depletion would attenuate protection (Figure 5C). However, BSO significantly exacerbated the toxicity of 6-OHDA in both control and MG132 treated cells to the same extent (29% BSO-induced drop in naïve cells and 31% drop in MG132 treated cells), failing to reduce the extent of MG132-induced protection against 6-OHDA (34% rise in viability in the absence of BSO and 32% rise in viability in the presence of BSO). BSO had no effect upon basal viability by itself in either group, as expected from the lack of effect upon α-tubulin signal noted above.

In order to ensure that BSO actually reduced GSH to the same extent in both control and MG132 treated cells, both groups were assayed for GSH after BSO ± 6-OHDA or their respective vehicles, 3, 6, and 24 hr later (Figure 5D–F). However, we found that the difference in GSH between naïve and MG132 pretreated cells was not statistically significant under any treatment condition. Indeed, BSO resulted in an approximately 60% loss of GSH at each time irrespective

of treatment group. At 24 hr, there was a significant 6-OHDA induced rise in GSH levels in control cells not treated with BSO, an effect of 6-OHDA which did not quite reach significance in cells treated with MG132 (Bonferroni post-hoc: $p = 0.08$) (Figure 5F).

CuZnSOD, MnSOD, catalase, and Hsp70 were higher in MG132 treated cells

6-OHDA has been shown to generate the superoxide radical (Heikkila and Cohen 1973) and is commonly used to model intracellular toxicity caused by oxidative stress. Therefore, protection against 6-OHDA might be expected to be provided by antioxidant enzymes, prominent among which are cytosolic CuZnSOD (Asanuma et al. 1998; Pong et al. 2000; Barkats et al. 2002), mitochondrial MnSOD (Callio et al. 2005), and catalase (Tiffany-Castiglioni et al. 1982; Hanrott et al. 2006; Saito et al. 2007). We thus began to determine whether these protective enzymes were higher in MG132 chronically-treated cells with immunoblotting, and found significantly higher levels of MnSOD (21%), CuZnSOD (55%), and catalase (15%) following MG132 treatment (Figure 6). Hsp 70 is known to rise upon cellular exposure to misfolded proteins, such as would be expected to occur after treatment with MG132 (Bush et al. 1997; Lee and Goldberg 1998b). Therefore, we also measured inducible Hsp 70 levels by immunoblotting, and found that levels of Hsp 70 were 42% higher in MG132 treated cells (Figure 6). In contrast, no significant change in another chaperone, Hsp 25, was observed (data not shown).

CuZnSOD downregulation by RNA interference attenuated MG132 induced protection against 6-OHDA

CuZnSOD has a high level of endogenous expression in nigral DA neurons (Zhang et al. 1993; Kunikowska and Jenner 2001, 2003), and has been shown to be protective against 6-OHDA (Asanuma et al. 1998; Pong et al. 2000; Barkats et al. 2002). We thus focused our attention on the next hypothesis that CuZnSOD played a key role in the protection afforded by MG132. First, we examined SOD activity to determine whether it increased in parallel to the MG132-induced increase observed in SOD proteins. We observed that CuZnSOD activity was increased by 40% (Figure 7A). This was not accompanied by a detectable change in MnSOD activity, suggesting that the modest rise in MnSOD apparent by immunoblotting was beyond the sensitivity of the activity assay or that it did not represent an increase of active protein. Cells harvested over the course of the initial 2 weeks in MG132 were also probed for CuZnSOD levels. A slow incremental rise was found – 100% for controls, 123% ± 10 at 4 days, 128% ± 9 at 8 days, and 147% ± 4 at >14 days spent in 0.1 μM MG132 (4 independent observations, $p<0.05$, Bonferroni post-hoc). Ubiquitin-conjugated protein levels also rose progressively, but with the higher variability also apparent in Figure 2 – 100% for controls, 111% ± 9 at 4 days, 121% ± 16 at 8 days, and 140% ± 25% for 14+ days (4 independent observations).

Finally, to test whether there was indeed a causal relationship between protection and CuZnSOD levels, we used RNA interference with two independent sequences. So as to minimize adverse effects upon basal viability by loss of a protective molecule, we strove to achieve knockdown only to the basal values of naïve control cells. For this, a small pilot immunoblotting study was undertaken to yield information on siRNA dose and knockdown temporal profile. Using these preliminary data it was determined with both sequences that 31 picomoles/cm^2 of siRNA reduced CuZnSOD levels in MG132 treated cells to near-control values at 24 hr (Figure 7B, C, left panels), the chosen time of 6-OHDA treatment for the viability experiments presented below.

For each sequence we repeated the siRNA knockdown for 6-OHDA toxicity studies with the same concentration (31 pmoles/cm^2 or 88 nM siRNA). 6-OHDA was administered at 200 μM due to increased confluence expected of the Lipofectamine protocol, 24 hr after siRNA treatment and cell viability was measured as usual 24 hr thereafter. Knockdown with either

sequence resulted in significant loss of MG132-induced protection against 6-OHDA, in that we observed a 32% drop with siRNA sequence 1 and a 27% drop with siRNA sequence 2 (Figure 7B, C, right panels). CuZnSOD knockdown thus rendered MG132 treated cells comparable to controls in their sensitivity to oxidative stress. Slight differences in viability between the two siRNA sequences may be attributable both to differences in siRNA transfection efficiency and in the toxicity of 6-OHDA and MG132 batches (see Methods). In contrast to findings with BSO where basal GSH levels were dropped by 60% (see Figure 5), the slight CuZnSOD knockdown in naïve controls with either sequence failed to significantly affect their response to 6-OHDA.

Discussion

Characterization of model and effect of MG132 on cellular resilience

We began by characterizing our new model of chronic stress. First, the MG132 treatment did not produce overt changes in cellular morphology or TH expression, nor were signs of neurite extension or differentiation observed over the course of 6 months. Second, we showed that MG132 in this paradigm inhibited chymotrypsin-like proteasome activity by 47%, as measured by a highly specific assay for the cytosolic 26S particle (Kisselev and Goldberg 2005). A statistical trend towards an average 42% rise in levels of ubiquitin-conjugated proteins was observed (two-tailed *p* value of 0.076, one-tailed *p* value of 0.038). Exposure to MG132 was then found to protect against 6-OHDA, with the protection developing over the course of 2 weeks. Protection was verified by two independent assays - cell counts (Hoechst-stained live nuclei) and an index of ATP levels (Cell Titer Glo). We also observed that chronic MG132 exposure decreased the toxic effects of a much higher concentration of MG132, a treatment which would not rely upon the DA transporter for inducing toxicity and was suggestive of non-specific "cross-tolerance" (see below). Finally, nomifensine-sensitive uptake through the high-affinity DA transporter was slightly increased by MG132 (36%). This latter finding suggested that any MG132-induced protection against 6-OHDA could not be readily explained by reductions in DA transporter function. In sum, the reduction in the toxic effects of both 6-OHDA and high-dose MG132 as measured by two independent assays is suggestive of a non-specific cross-tolerance against multiple types of injury. Interestingly, a previous preconditioning study of ours showed that acute sublethal 6-OHDA also induced cross-tolerance against normally toxic levels of MG132 (Leak et al. 2006).

The possible involvement of cathepsins and calpains, in addition to the proteasome, in our MG132 model system would be expected to increase damaged proteins and cellular stress as well, and was not viewed as undesirable for our particular questions. Nevertheless, in preliminary studies we also found that epoxomicin, still believed to be more specific than MG132, elicited protection against 6-OHDA, but within a narrow range of concentration (~1.25 nM). This is consistent with previous work showing that epoxomicin and lactacystin are protective against oxidative insults in other models (Lee et al. 2004; van Leyen et al. 2005), although these other models did not involve chronic pretreatments. At higher doses (>2.5 nM) epoxomicin led to cell death of the entire population over the course of 2 or more weeks. We emphasize here that in our model, high enough stress levels are expected to cause an *exacerbation* of toxicity instead of protection, in an inverted U-shaped dose-response curve. For example, one study on SH-SY5Y cells noted that 200 μM MG132 potentiated 50 μM 6-OHDA toxicity (Elkon et al. 2001). In PC12 cells, we similarly found that higher concentrations of MG132 (4 μM) actually exacerbated 6-OHDA toxicity, doubling the drop in viability after 50 μM 6-OHDA (19% loss in ATP in control cells and 40% loss with high dose MG132).

In our PC12 model, in contrast to long-term exposures to MG132 of 14 days or longer, short-term, 24 hr exposure was insufficient to elicit any protection, and protection was sub-maximal with exposure to 4 and 8 days of MG132. Protection was still apparent 48 hr after removal of

the 6-OHDA challenge. In contrast, removal of the MG132 stimulus for 14 days resulted in a complete loss of acquired adaptive defenses and a reversal to the original state of vulnerability to 6-OHDA. These data suggest that the effect does not appear to represent delay of inevitable 6-OHDA-induced cell death but that the stimulus must be prolonged and maintained for this adaptive response.

Mechanism of protection against 6-OHDA

In an effort to determine the mechanism underlying the protection against ROS conferred by chronic MG132, we first examined GSH antioxidant defenses. We observed that 100 μM BSO, which reduced overall GSH levels by 60%, did not affect the degree of MG132-induced protection against 6-OHDA at all. Instead, it successfully enhanced the toxicity of 6-OHDA in both control and MG132 treated cells by almost precisely the same extent, showing that the overall levels of GSH were not simply in excess of cellular requirements in this paradigm. 6-OHDA treatment caused a slight increase in GSH levels in naïve cells 24 hr following removal, perhaps as an adaptive response to oxidative injury. In contrast, MG132 did not cause a significant change in GSH levels from that of control cells under any treatment condition. Therefore, we conclude that GSH was equally important for defense against oxidative stress in both control and MG132 treated groups, and that protection arising from MG132 exposure *per se* was unrelated to GSH. These findings are important in light of the well-known drop in GSH levels in the substantia nigra in early PD (Dexter et al. 1994), and illustrate that cells, at least initially, are able to rely upon alternate pathways for adaptive defenses in the face of extensive GSH loss.

Next, we examined four well-known defensive proteins - catalase, MnSOD, CuZnSOD and Hsp 70, and found levels of each to be significantly higher in MG132 treated cells. No significant changes in Hsp 25 or TH levels argue against global, non-specific changes. In our study we have no evidence regarding whether the above changes represent an increase in protein synthesis, a decrease in protein degradation, or both. However, microarray studies have shown transcriptional changes with proteasome inhibitors (Yew et al. 2005), and previous studies reported an increase in Hsp mRNA with MG132 (Bush et al. 1997; Lee and Goldberg 1998b). Furthermore, a recent *Arabidopsis* study revealed that microRNA suppression of CuZnSOD gene expression is released by oxidative stress and plays a critical role in the subsequent induction of stress-induced tolerance (Sunkar et al. 2006).

As blotting revealed a trend towards a rise in ubiquitinated proteins, which could have included CuZnSOD (Kabuta et al. 2006), one might wonder whether the defensive proteins assayed were actually functional. This hypothesis was inconsistent with our observations that functional enzyme activity levels of CuZnSOD were higher with MG132 and that knockdown of CuZnSOD with each of two independent siRNA sequences attenuated protection. We reasoned that knockdown of CuZnSOD levels to approximate that of naïve controls would minimize adverse effects upon basal viability and allow some CuZnSOD to be present for normal homeostatic function. This strategy also allowed us to test whether similar 6-OHDA induced toxicity values would then arise as in controls. Overall, the data support the hypothesis that CuZnSOD, but not GSH, mediated chronic MG132-induced protection. Whether catalase and Hsp 70 similarly contribute to chronic stress-induced protection remains to be determined.

Prior studies have used virally-mediated or transgenic overexpression of CuZnSOD to examine whether this protein can be protective in models of PD (Przedborski et al. 1992; Asanuma et al. 1998; Barkats et al. 2002; Barkats et al. 2006; Choi et al. 2006; Wang et al. 2006). One *in vivo* study of CuZnSOD knockouts showed increased DA terminal degeneration in a PD model (Zhang et al. 2000). Our present study extends such observations by indicating that dopaminergic cells faced with long-term stress also use this enzyme for *endogenous* self-defense. There is a prominent loss of CuZnSOD mRNA from the ventral midbrain in 6-OHDA-

treated rats, MPTP-treated monkeys, and human PD (Kunikowska and Jenner 20012003), as well as anatomical observations of high endogenous expression of CuZnSOD within melanized human DA neurons (Zhang et al. 1993). Thus, it can be speculated that endogenous CuZnSOD plays a critical role in self-protecting DA neurons. Whether this enzyme is higher in DA cells experiencing high levels of damaged proteins *in vivo* is not clear, but with our novel findings we suggest that CuZnSOD is worthy of detailed characterization across all the brain regions exhibiting synuclein-positive inclusions, preferably as a function of the Braak staging of PD (Braak et al. 2003).

Implications for *in vivo* studies of proteasome inhibition

Studies involving the intracerebral administration of proteasome inhibitors typically find dopaminergic cell death rather than protection (Fornai et al. 2003; McNaught et al. 2003; McNaught 2004; Miwa et al. 2005; Schapira et al. 2006; Sun et al. 2006), although a large number of studies with systemic treatments failed to find toxicity (Beal and Lang 2006). In contrast, a few studies actually show protection of DA neurons with intracerebral proteasome inhibitors (Sawada et al. 2004; Inden et al. 2005). Such varying effects of proteasome inhibitors have been discussed as concentration-dependent, with low doses eliciting adaptive responses (Lin et al. 1998; Sawada et al. 2004; Setsuie et al. 2005) as seen in the present study. Our findings also carry some implications for the use of proteasome inhibitors in cancer treatment (Zavrski et al. 2007), for they suggest that there may be a “paradoxical” resilience in those tumor cells that fail to experience high enough concentrations of the drug.

Conclusions

The motor symptoms of PD progress slowly despite a reduction in nigral proteasome activity (McNaught et al. 2003). The present report examined whether PC12 cells might adapt to chronic MG132, a treatment that dropped chymotrypsin activity by 47% and was expected to increase levels of cellular stress. MG132 at a sublethal dose of 0.1 μM did not appear to affect cell growth rates and rendered PC12 cells resistant to both the oxidative toxicity of 6-OHDA (100 and 200 μM) and to normally lethal concentrations of MG132 (40 μM). The decrease in 6-OHDA vulnerability was independent of GSH but was associated with higher levels of several defensive proteins. Evidence was then obtained suggesting that enzymatically active CuZnSOD played a key role in MG132-induced resilience to oxidative stress. When considered together with similar reports in the literature, these data indicate that the ability to mount defensive responses to injury is a fundamental and intrinsic cellular property. Whether similar adaptations serve to reduce the incidence of neurodegenerative diseases and delay its appearance in those that develop such conditions in their older years deserves further examination. Our results also raise the possibility that increasing endogenous defenses through drug treatment or gene therapy will delay the progression of such illnesses even further.

Acknowledgments

The research described herein was supported by grants from the National Institute of Neurological Disorders and Stroke (NS19608) and the U.S. Army (ERMS#03281022) to MJZ. We thank Donald B. DeFranco, Juliann D. Jaumotte, and Ruth G. Perez for helpful discussions, and Gonzalo E. Torres for providing stably transfected PC12 cells.

List of Abbreviations

6-OHDA	6-hydroxydopamine
BCA	bicinchoninic acid
BSO	buthionine sulfoximine
DMSO	dimethyl sulfoxide

DA	dopamine
GSH	glutathione
Hsp	heat shock protein
PD	Parkinson's disease
ROS	reactive oxygen species
SOD	superoxide dismutase
TH	tyrosine hydroxylase

References

Asanuma M, Hirata H, Cadet JL. Attenuation of 6-hydroxydopamine-induced dopaminergic nigrostriatal lesions in superoxide dismutase transgenic mice. Neuroscience 1998;85:907–917. [PubMed: 9639283]

Barkats M, Millecamps S, Bilang-Bleuel A, Mallet J. Neuronal transfer of the human Cu/Zn superoxide dismutase gene increases the resistance of dopaminergic neurons to 6-hydroxydopamine. J Neurochem 2002;82:101–109. [PubMed: 12091470]

Barkats M, Horellou P, Colin P, Millecamps S, Faucon-Biguet N, Mallet J. 1-methyl-4-phenylpyridinium neurotoxicity is attenuated by adenoviral gene transfer of human Cu/Zn superoxide dismutase. J Neurosci Res 2006;83:233–242. [PubMed: 16353238]

Beal F, Lang A. The proteasomal inhibition model of Parkinson's disease: "Boon or bust"? Ann Neurol 2006;60:158–161. [PubMed: 16862578]

Braak H, Del Tredici K, Rub U, de Vos RA, Jansen Steur EN, Braak E. Staging of brain pathology related to sporadic Parkinson's disease. Neurobiol Aging 2003;24:197–211. [PubMed: 12498954]

Bush KT, Goldberg AL, Nigam SK. Proteasome inhibition leads to a heat-shock response, induction of endoplasmic reticulum chaperones, and thermotolerance. J Biol Chem 1997;272:9086–9092. [PubMed: 9083035]

Callio J, Oury TD, Chu CT. Manganese superoxide dismutase protects against 6-hydroxydopamine injury in mouse brains. J Biol Chem 2005;280:18536–18542. [PubMed: 15755737]

Choi HS, An JJ, Kim SY, Lee SH, Kim DW, Yoo KY, Won MH, Kang TC, Kwon HJ, Kang JH, Cho SW, Kwon OS, Park J, Eum WS, Choi SY. PEP-1-SOD fusion protein efficiently protects against paraquat-induced dopaminergic neuron damage in a Parkinson disease mouse model. Free Radic Biol Med 2006;41:1058–1068. [PubMed: 16962931]

Clement MV, Long LH, Ramalingam J, Halliwell B. The cytotoxicity of dopamine may be an artefact of cell culture. J Neurochem 2002;81:414–421. [PubMed: 12065650]

Conconi M, Szweda LI, Levine RL, Stadtman ER, Friguet B. Age-related decline of rat liver multicatalytic proteinase activity and protection from oxidative inactivation by heat-shock protein 90. Arch Biochem Biophys 1996;331:232–240. [PubMed: 8660703]

Dexter DT, Sian J, Rose S, Hindmarsh JG, Mann VM, Cooper JM, Wells FR, Daniel SE, Lees AJ, Schapira AH, et al. Indices of oxidative stress and mitochondrial function in individuals with incidental Lewy body disease. Ann Neurol 1994;35:38–44. [PubMed: 8285590]

Ding Q, Dimayuga E, Martin S, Bruce-Keller AJ, Nukala V, Cuervo AM, Keller JN. Characterization of chronic low-level proteasome inhibition on neural homeostasis. J Neurochem 2003;86:489–497. [PubMed: 12871590]

Ding YM, Jaumotte JD, Signore AP, Zigmond MJ. Effects of 6-hydroxydopamine on primary cultures of substantia nigra: specific damage to dopamine neurons and the impact of glial cell line-derived neurotrophic factor. J Neurochem 2004;89:776–787. [PubMed: 15086533]

Elkon H, Melamed E, Offen D. 6-Hydroxydopamine increases ubiquitin-conjugates and protein degradation: implications for the pathogenesis of Parkinson's disease. Cell Mol Neurobiol 2001;21:771–781. [PubMed: 12043847]

Fornai F, Lenzi P, Gesi M, Ferrucci M, Lazzeri G, Busceti CL, Ruffoli R, Soldani P, Ruggieri S, Alessandri MG, Paparelli A. Fine structure and biochemical mechanisms underlying nigrostriatal

inclusions and cell death after proteasome inhibition. J Neurosci 2003;23:8955–8966. [PubMed: 14523098]

Friguet B, Bulteau AL, Chondrogianni N, Conconi M, Petropoulos I. Protein degradation by the proteasome and its implications in aging. Ann N Y Acad Sci 2000;908:143–154. [PubMed: 10911955]

Fuertes G, Martin De Llano JJ, Villarroya A, Rivett AJ, Knecht E. Changes in the proteolytic activities of proteasomes and lysosomes in human fibroblasts produced by serum withdrawal, amino-acid deprivation and confluent conditions. Biochem J 2003;375:75–86. [PubMed: 12841850]

Fujimuro M, Sawada H, Yokosawa H. Production and characterization of monoclonal antibodies specific to multi-ubiquitin chains of polyubiquitinated proteins. FEBS Lett 1994;349:173–180. [PubMed: 7519568]

Hanrott K, Gudmunsen L, O'Neill MJ, Wonnacott S. 6-hydroxydopamine-induced apoptosis is mediated via extracellular auto-oxidation and caspase 3-dependent activation of protein kinase Cdelta. J Biol Chem 2006;281:5373–5382. [PubMed: 16361258]

Heikkila RE, Cohen G. 6-Hydroxydopamine: evidence for superoxide radical as an oxidative intermediate. Science 1973;181:456–457. [PubMed: 4718113]

Inden M, Kondo J, Kitamura Y, Takata K, Nishimura K, Taniguchi T, Sawada H, Shimohama S. Proteasome inhibitors protect against degeneration of nigral dopaminergic neurons in hemiparkinsonian rats. Journal of pharmacological sciences 2005;97:203–211. [PubMed: 15684568]

Kabuta T, Suzuki Y, Wada K. Degradation of amyotrophic lateral sclerosis-linked mutant Cu,Zn-superoxide dismutase proteins by macroautophagy and the proteasome. J Biol Chem 2006;281:30524–30533. [PubMed: 16920710]

Keck S, Nitsch R, Grune T, Ullrich O. Proteasome inhibition by paired helical filament-tau in brains of patients with Alzheimer's disease. J Neurochem 2003;85:115–122. [PubMed: 12641733]

Keller JN, Hanni KB, Markesbery WR. Impaired proteasome function in Alzheimer's disease. J Neurochem 2000a;75:436–439. [PubMed: 10854289]

Keller JN, Huang FF, Markesbery WR. Decreased levels of proteasome activity and proteasome expression in aging spinal cord. Neuroscience 2000b;98:149–156. [PubMed: 10858621]

Kisselev AF, Goldberg AL. Proteasome inhibitors: from research tools to drug candidates. Chemistry & biology 2001;8:739–758. [PubMed: 11514224]

Kisselev AF, Goldberg AL. Monitoring activity and inhibition of 26S proteasomes with fluorogenic peptide substrates. Methods in enzymology 2005;398:364–378. [PubMed: 16275343]

Kitagawa K, Matsumoto M, Tagaya M, Hata R, Ueda H, Niinobe M, Handa N, Fukunaga R, Kimura K, Mikoshiba K, et al. 'Ischemic tolerance' phenomenon found in the brain. Brain Res 1990;528:21–24. [PubMed: 2245337]

Kunikowska G, Jenner P. 6-Hydroxydopamine-lesioning of the nigrostriatal pathway in rats alters basal ganglia mRNA for copper, zinc- and manganese-superoxide dismutase, but not glutathione peroxidase. Brain Res 2001;922:51–64. [PubMed: 11730701]

Kunikowska G, Jenner P. Alterations in m-RNA expression for Cu,Zn-superoxide dismutase and glutathione peroxidase in the basal ganglia of MPTP-treated marmosets and patients with Parkinson's disease. Brain Res 2003;968:206–218. [PubMed: 12663090]

Leak RK, Liou AK, Zigmond MJ. Effect of sublethal 6-hydroxydopamine on the response to subsequent oxidative stress in dopaminergic cells: evidence for preconditioning. J Neurochem 2006;99:1151–1163. [PubMed: 16956375]

Lee CS, Tee LY, Warmke T, Vinjamoori A, Cai A, Fagan AM, Snider BJ. A proteasomal stress response: pre-treatment with proteasome inhibitors increases proteasome activity and reduces neuronal vulnerability to oxidative injury. J Neurochem 2004;91:996–1006. [PubMed: 15525353]

Lee DH, Goldberg AL. Proteasome inhibitors: valuable new tools for cell biologists. Trends Cell Biol 1998a;8:397–403. [PubMed: 9789328]

Lee DH, Goldberg AL. Proteasome inhibitors cause induction of heat shock proteins and trehalose, which together confer thermotolerance in Saccharomyces cerevisiae. Mol Cell Biol 1998b;18:30–38. [PubMed: 9418850]

Lin E, Cavanaugh JE, Leak RK, Perez RG, Zigmond MJ. Rapid activation of ERK by 6-hydroxydopamine promotes survival of dopaminergic cells. J Neurosci Res 2008;86:108–117. [PubMed: 17847117]

Lin KI, Baraban JM, Ratan RR. Inhibition versus induction of apoptosis by proteasome inhibitors depends on concentration. Cell Death Differ 1998;5:577–583. [PubMed: 10200512]

Lopez Salon M, Morelli L, Castano EM, Soto EF, Pasquini JM. Defective ubiquitination of cerebral proteins in Alzheimer's disease. J Neurosci Res 2000;62:302–310. [PubMed: 11020223]

McNaught KS. Proteolytic dysfunction in neurodegenerative disorders. International review of neurobiology 2004;62:95–119. [PubMed: 15530569]

McNaught KS, Belizaire R, Isacson O, Jenner P, Olanow CW. Altered proteasomal function in sporadic Parkinson's disease. Exp Neurol 2003;179:38–46. [PubMed: 12504866]

McNaught KS, Bjorklund LM, Belizaire R, Isacson O, Jenner P, Olanow CW. Proteasome inhibition causes nigral degeneration with inclusion bodies in rats. Neuroreport 2002;13:1437–1441. [PubMed: 12167769]

Merker K, Stolzing A, Grune T. Proteolysis, caloric restriction and aging. Mechanisms of ageing and development 2001;122:595–615. [PubMed: 11322989]

Miwa H, Kubo T, Suzuki A, Nishi K, Kondo T. Retrograde dopaminergic neuron degeneration following intrastriatal proteasome inhibition. Neurosci Lett 2005;380:93–98. [PubMed: 15854758]

Murry CE, Jennings RB, Reimer KA. Preconditioning with ischemia: a delay of lethal cell injury in ischemic myocardium. Circulation 1986;74:1124–1136. [PubMed: 3769170]

Mytilineou C, McNaught KS, Shashidharan P, Yabut J, Baptiste RJ, Parnandi A, Olanow CW. Inhibition of proteasome activity sensitizes dopamine neurons to protein alterations and oxidative stress. J Neural Transm 2004;111:1237–1251. [PubMed: 15480836]

Ohtake F, Baba A, Takada I, Okada M, Iwasaki K, Miki H, Takahashi S, Kouzmenko A, Nohara K, Chiba T, Fujii-Kuriyama Y, Kato S. Dioxin receptor is a ligand-dependent E3 ubiquitin ligase. Nature 2007;446:562–566. [PubMed: 17392787]

Pong K, Doctrow SR, Baudry M. Prevention of 1-methyl-4-phenylpyridinium- and 6-hydroxydopamine-induced nitration of tyrosine hydroxylase and neurotoxicity by EUK-134, a superoxide dismutase and catalase mimetic, in cultured dopaminergic neurons. Brain Res 2000;881:182–189. [PubMed: 11036157]

Przedborski S, Kostic V, Jackson-Lewis V, Naini AB, Simonetti S, Fahn S, Carlson E, Epstein CJ, Cadet JL. Transgenic mice with increased Cu/Zn-superoxide dismutase activity are resistant to N-methyl-4-phenyl-1,2,3,6-tetrahydropyridine-induced neurotoxicity. J Neurosci 1992;12:1658–1667. [PubMed: 1578260]

Rideout HJ, Lang-Rollin IC, Savalle M, Stefanis L. Dopaminergic neurons in rat ventral midbrain cultures undergo selective apoptosis and form inclusions, but do not up-regulate iHSP70, following proteasomal inhibition. J Neurochem 2005;93:1304–1313. [PubMed: 15934949]

Rideout HJ, Larsen KE, Sulzer D, Stefanis L. Proteasomal inhibition leads to formation of ubiquitin/alpha-synuclein-immunoreactive inclusions in PC12 cells. J Neurochem 2001;78:899–908. [PubMed: 11520910]

Rodgers KJ, Dean RT. Assessment of proteasome activity in cell lysates and tissue homogenates using peptide substrates. Int J Biochem Cell Biol 2003;35:716–727. [PubMed: 12672463]

Saggu H, Cooksey J, Dexter D, Wells FR, Lees A, Jenner P, Marsden CD. A selective increase in particulate superoxide dismutase activity in parkinsonian substantia nigra. J Neurochem 1989;53:692–697. [PubMed: 2760616]

Saito Y, Nishio K, Ogawa Y, Kinumi T, Yoshida Y, Masuo Y, Niki E. Molecular mechanisms of 6-hydroxydopamine-induced cytotoxicity in PC12 cells: involvement of hydrogen peroxide-dependent and -independent action. Free Radic Biol Med 2007;42:675–685. [PubMed: 17291991]

Sawada H, Kohno R, Kihara T, Izumi Y, Sakka N, Ibi M, Nakanishi M, Nakamizo T, Yamakawa K, Shibasaki H, Yamamoto N, Akaike A, Inden M, Kitamura Y, Taniguchi T, Shimohama S. Proteasome mediates dopaminergic neuronal degeneration, and its inhibition causes alpha-synuclein inclusions. J Biol Chem 2004;279:10710–10719. [PubMed: 14672949]

Schapira AH, Cleeter MW, Muddle JR, Workman JM, Cooper JM, King RH. Proteasomal inhibition causes loss of nigral tyrosine hydroxylase neurons. Ann Neurol 2006;60:253–255. [PubMed: 16862591]

Setsuie R, Kabuta T, Wada K. Does proteasome [corrected] inhibition decrease or accelerate toxin-induced dopaminergic neurodegeneration? Journal of pharmacological sciences 2005;97:457–460. [PubMed: 15764834]

Sun F, Anantharam V, Zhang D, Latchoumycandane C, Kanthasamy A, Kanthasamy AG. Proteasome inhibitor MG-132 induces dopaminergic degeneration in cell culture and animal models. Neurotoxicology 2006;27:807–815. [PubMed: 16870259]

Sunkar R, Kapoor A, Zhu JK. Posttranscriptional induction of two Cu/Zn superoxide dismutase genes in Arabidopsis is mediated by downregulation of miR398 and important for oxidative stress tolerance. The Plant cell 2006;18:2051–2065. [PubMed: 16861386]

Tiffany-Castiglioni E, Saneto RP, Proctor PH, Perez-Polo JR. Participation of active oxygen species in 6-hydroxydopamine toxicity to a human neuroblastoma cell line. Biochem Pharmacol 1982;31:181–188. [PubMed: 7059360]

van Leyen K, Siddiq A, Ratan RR, Lo EH. Proteasome inhibition protects HT22 neuronal cells from oxidative glutamate toxicity. J Neurochem 2005;92:824–830. [PubMed: 15686484]

Wang D, Qian L, Xiong H, Liu J, Neckameyer WS, Oldham S, Xia K, Wang J, Bodmer R, Zhang Z. Antioxidants protect PINK1-dependent dopaminergic neurons in Drosophila. Proc Natl Acad Sci U S A 2006;103:13520–13525. [PubMed: 16938835]

Yamamoto N, Sawada H, Izumi Y, Kume T, Katsuki H, Shimohama S, Akaike A. Proteasome inhibition induces glutathione synthesis and protects cells from oxidative stress: relevance to Parkinson disease. J Biol Chem 2007;282:4364–4372. [PubMed: 17158454]

Yew EH, Cheung NS, Choy MS, Qi RZ, Lee AY, Peng ZF, Melendez AJ, Manikandan J, Koay ES, Chiu LL, Ng WL, Whiteman M, Kandiah J, Halliwell B. Proteasome inhibition by lactacystin in primary neuronal cells induces both potentially neuroprotective and pro-apoptotic transcriptional responses: a microarray analysis. J Neurochem 2005;94:943–956. [PubMed: 15992382]

Zavrski I, Jakob C, Kaiser M, Fleissner C, Heider U, Sezer O. Molecular and clinical aspects of proteasome inhibition in the treatment of cancer. Recent Results Cancer Res 2007;176:165–176. [PubMed: 17607924]

Zhang J, Graham DG, Montine TJ, Ho YS. Enhanced N-methyl-4-phenyl-1,2,3,6-tetrahydropyridine toxicity in mice deficient in CuZn-superoxide dismutase or glutathione peroxidase. J Neuropathol Exp Neurol 2000;59:53–61. [PubMed: 10744035]

Zhang P, Damier P, Hirsch EC, Agid Y, Ceballos-Picot I, Sinet PM, Nicole A, Laurent M, Javoy-Agid F. Preferential expression of superoxide dismutase messenger RNA in melanized neurons in human mesencephalon. Neuroscience 1993;55:167–175. [PubMed: 8350985]

Zigmond, MJ.; Keefe, K. 6-Hydroxydopamine as a tool for studying catecholamines in adult animals: lessons from the neostriatum. Humana Press; Totowa, NJ: 1997. p. 75-108.

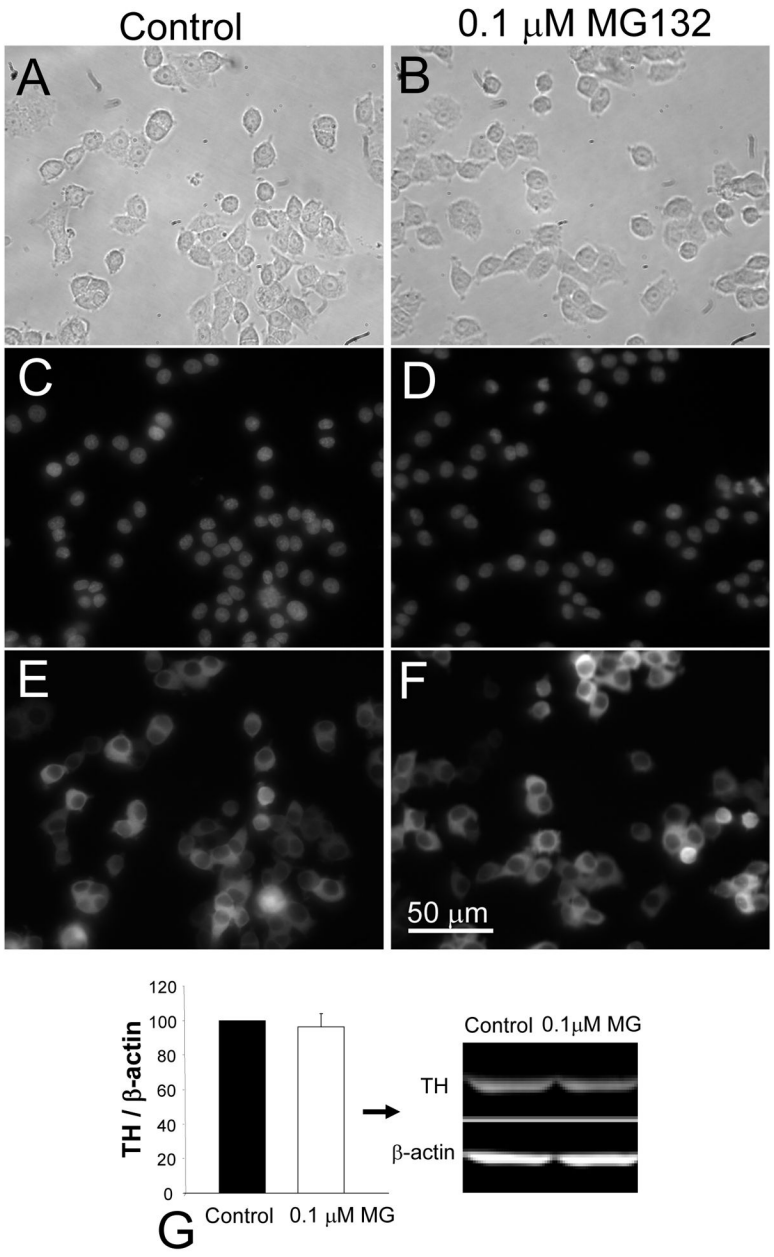

Figure 1. Chronic MG132 treatment did not affect morphological appearance of PC12 cells

Brightfield (**A, B**), Hoechst staining (**C, D**) and TH immunolabeling (**E, F**) of naïve control (**A, C, E**) versus chronic MG132-treated cells (**B, D, F**). Cells were fixed and stained 48 hr after side-by-side passaging and plating at equal densities. Images were captured at the same exposure settings for both groups. Immunoblotting verified the lack of effect upon levels of TH protein (**G**). Total TH levels were expressed as a fraction of β-actin label to control for variations in protein loading and presented as mean + SEM from 6 independent experiments. Scale bar denotes 50 μm in A–F.

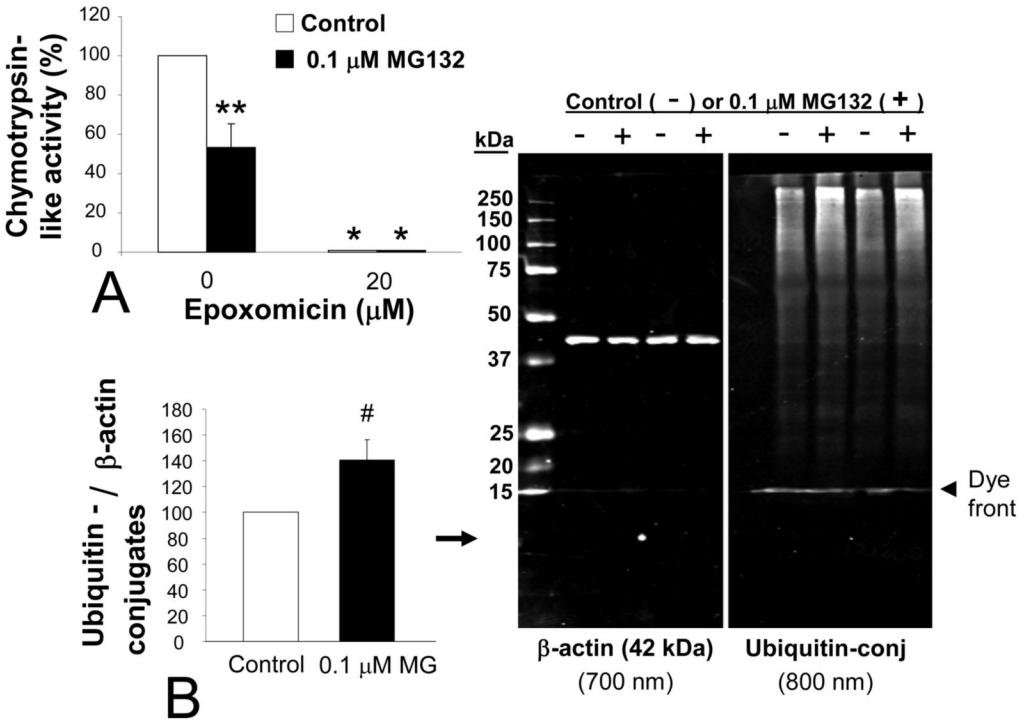

Figure 2. Chronic MG132 decreased proteasome activity levels

(**A**) Fluorescent reporting of cleavage of Suc-LLVY-amc, substrate for assaying chymotrypsin-like proteasome activity, without (white bars) and with (black bars) chronic treatment of MG132. Treatment of duplicate samples with epoxomicin *during* the assay effectively dropped all fluorescence values and acted as a negative control. Bonferroni post-hoc: *$p<0.05$ versus same group without epoxomicin, **$p<0.05$ versus adjacent white bar of naïve control cells. (**B**) Levels of ubiquitin-conjugated proteins in PC12 cells with and without chronic MG132 are shown with 250 to 15 kDa standards visible in the 700 nm channel next to the β-actin loading controls. The blue Laemmli buffer's dye front is visible in both fluorescent channels, but appears greater at 800 nm because a better signal:noise ratio of the β-actin antibody allows scanning at a lower setting. Two sets harvested maximally far apart (6 months) are illustrated. Two-tailed t-test: # $p=0.076$ versus white bar of naïve control cells. Data in A and B are presented as mean + SEM from 3–7 independent experiments.

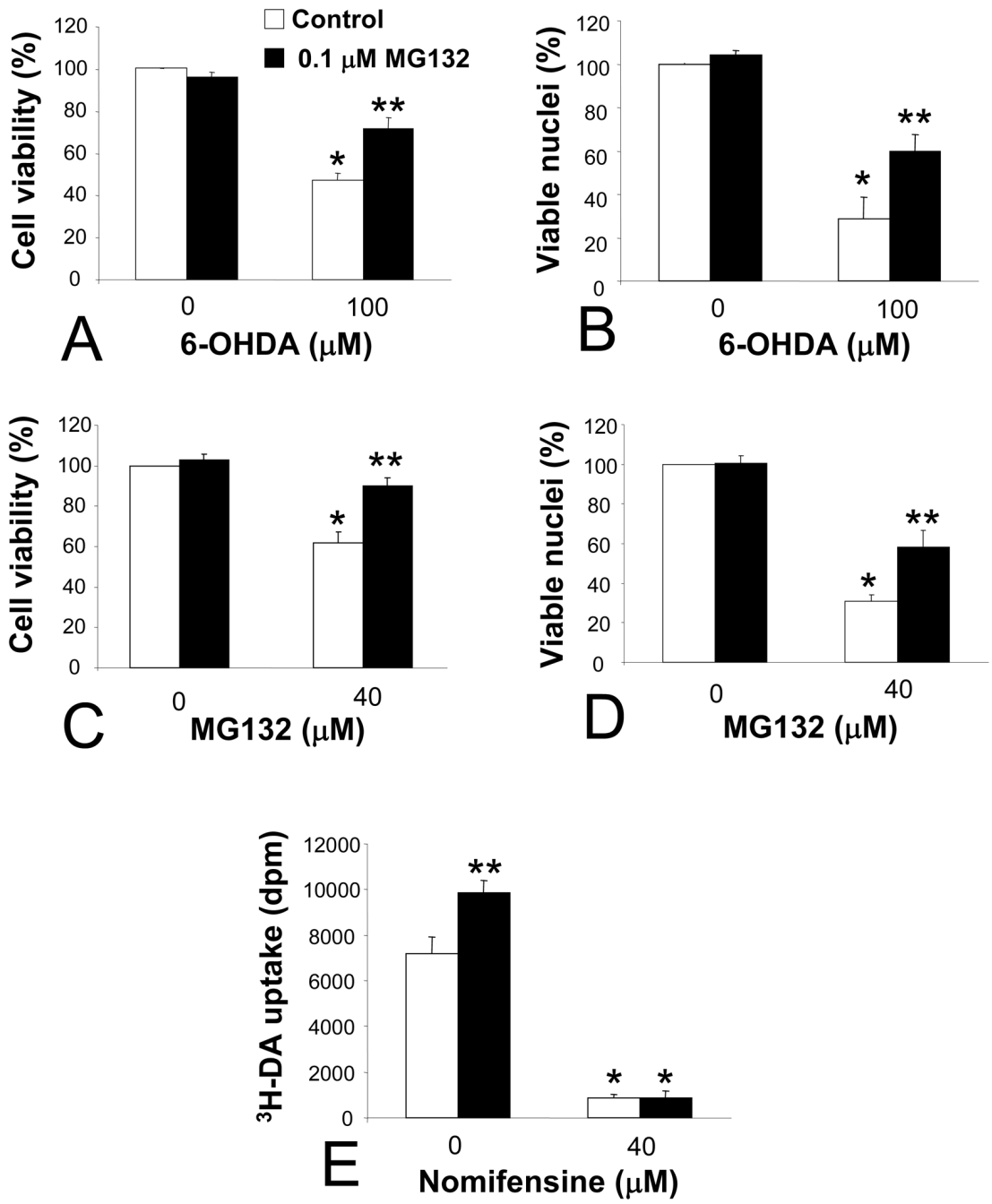

Figure 3. Chronic MG132 protected against two different types of cellular injury and increased transport of tritiated dopamine (^{3}H-DA) across the membrane

(**A–D**) MG132 treatment protected against both 6-OHDA and a high concentration of MG132. Viability was assessed by measuring ATP levels with Cell Titer Glo (**A, C**) or by counting Hoechst-positive viable nuclei (**B, D**). Cells were treated with vehicle or 6-OHDA (**A, B**) and DMSO or MG132 (**C, D**) at indicated concentrations, and assayed 24 hr thereafter. (**E**) ^{3}H-DA uptake in control and MG132 treated cells, with and without high-affinity dopamine transport blocker nomifensine (negative control applied *during* assay). Bonferroni post-hoc following ANOVA: **p*<0.05 versus same group without 6-OHDA or without high dose MG132 treatment in **A–D**, **p*<0.05 versus same group without nomifensine in **E**, ** *p*<0.05 versus white bar of

naïve control cells in **A–E**. Data are presented as mean + SEM from 3–5 independent experiments.

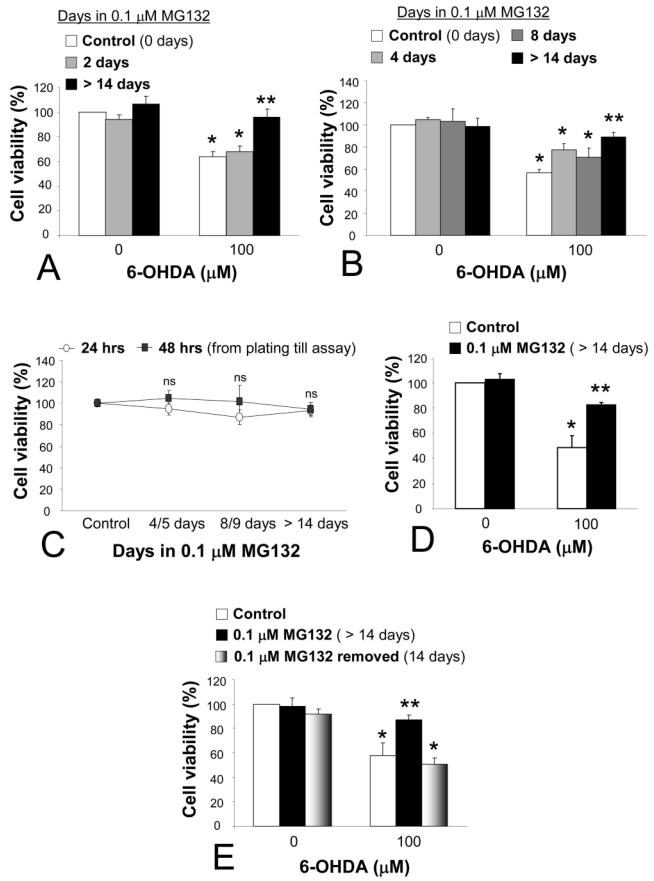

Figure 4. MG132 needed to be chronic and maintained in order to elicit maximal protection

(**A**) Naïve control cells were pretreated for 24 hr with 0.1 μM MG132, and then MG132 was also present during and after 6-OHDA (additional 24.5 hr). Cells were assayed for cellular viability 24 hr after 6-OHDA removal (48.5 total hr of MG132 for gray bars). Side-by-side experiments on control (white bars) and chronic MG132-treated (>14 days, black bars) cells serve as negative and positive controls to verify long term MG132-induced protection against 6-OHDA toxicity. (**B**) Growing PC12 cells for 4 days (light gray) and 8 days (dark gray) in MG132 prior to 6-OHDA exposure elicited sub-maximal protection relative to >14 days exposure (black bars). Cells were assayed 24 hrs after 6-OHDA removal. (**C**) Basal viability was not affected by the 0.1 μM dose of MG132, as measured at multiple timepoints. Cells grown for 4/5, 8/9, or >14 days in MG132 did not exhibit differences in cell density over the course of 24 or 48 hrs from time of plating (at 3, 7, and 14+ days) until assay 24 or 48 hrs later. ns = not significant. See text for details. (**D**) Assaying 48 hrs after removal of 6-OHDA challenge revealed continued, robust protection against 6-OHDA toxicity. (**E**) Removing MG132 for 2 weeks (bars with gray gradient) caused a reversal back to the original 6-OHDA vulnerability. Experiments on control and chronic MG132-treated cells verified protection against 6-OHDA toxicity in the same experiments. All viability measures in A–E were performed with Cell Titer Glo. Data are presented as mean + SEM from 3–4 independent experiments. Bonferroni post-hoc following ANOVA: *p<0.05 versus same group without 6-OHDA, **p<0.05 versus white bar denoting naïve control cells.

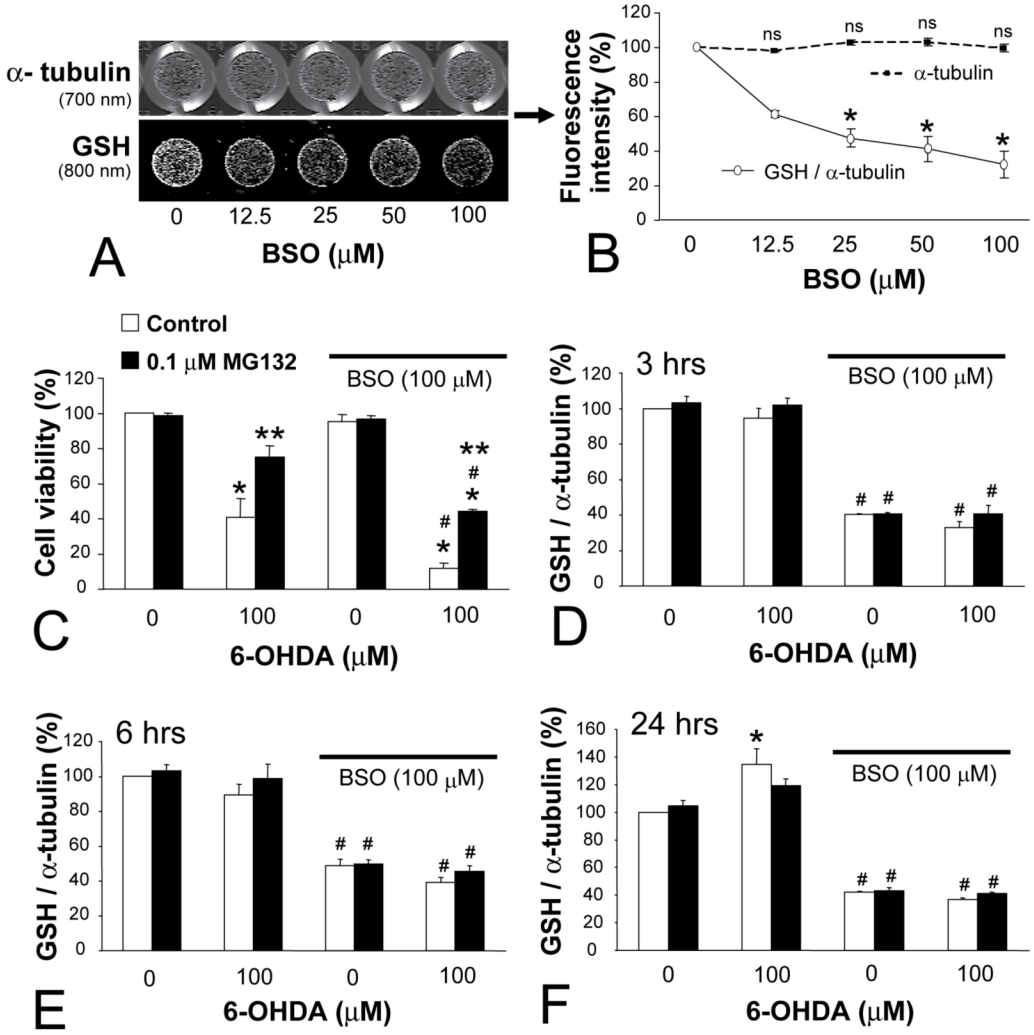

Figure 5. Glutathione (GSH) depletion did not attenuate protection conferred by chronic MG132

(**A**) Development of infrared In-Cell Western assay for total GSH levels, showing same plate wells dual-stained for mouse anti-α-tubulin primary (labeled with 700 nm goat anti-mouse secondary) and rabbit anti-total GSH primary (800 nm goat anti-rabbit secondary). Note that measurements are of the interior of each well, which excludes the background fluorescence of the walls in the 700 nm channel. GSH levels dropped with increasing concentrations of buthionine sulfoximine (BSO, 24 hr) without similar effect upon α-tubulin levels at these doses. Quantification of GSH (solid line, white circles) and α-tubulin levels (dashed line, black squares) is depicted in (**B**). GSH is expressed as a percentage of α-tubulin levels within the same wells across 3 independent experiments. (**C**) BSO exacerbated 6-OHDA toxicity but did not affect the degree of protection conferred by MG132. Cells were treated with BSO (all bars under solid black line) or an equal volume of PBS (remaining bars) for 24 hr before 6-OHDA or vehicle (30 min). 6-OHDA was removed and cells then left in BSO for an additional 24 hr before viability assay with Cell Titer Glo. (**D**–**F**) show In-Cell Western data for GSH levels at 3, 6, and 24 hr after 6-OHDA removal. Cells were treated precisely in the same format as in (**C**). MG132 did not increase GSH levels and BSO depleted GSH to the same extent in both naïve control and MG132 treated cells at every timepoint. Data are mean + SEM from 3–4 independent experiments. Bonferroni post-hoc following ANOVA: * $p<0.05$ versus no BSO

in **B** and versus same group without 6-OHDA in **C–F**, ** $p<0.05$ versus adjacent white bar of naïve control cells, # $p<0.05$ versus same group without BSO in **C–F**.

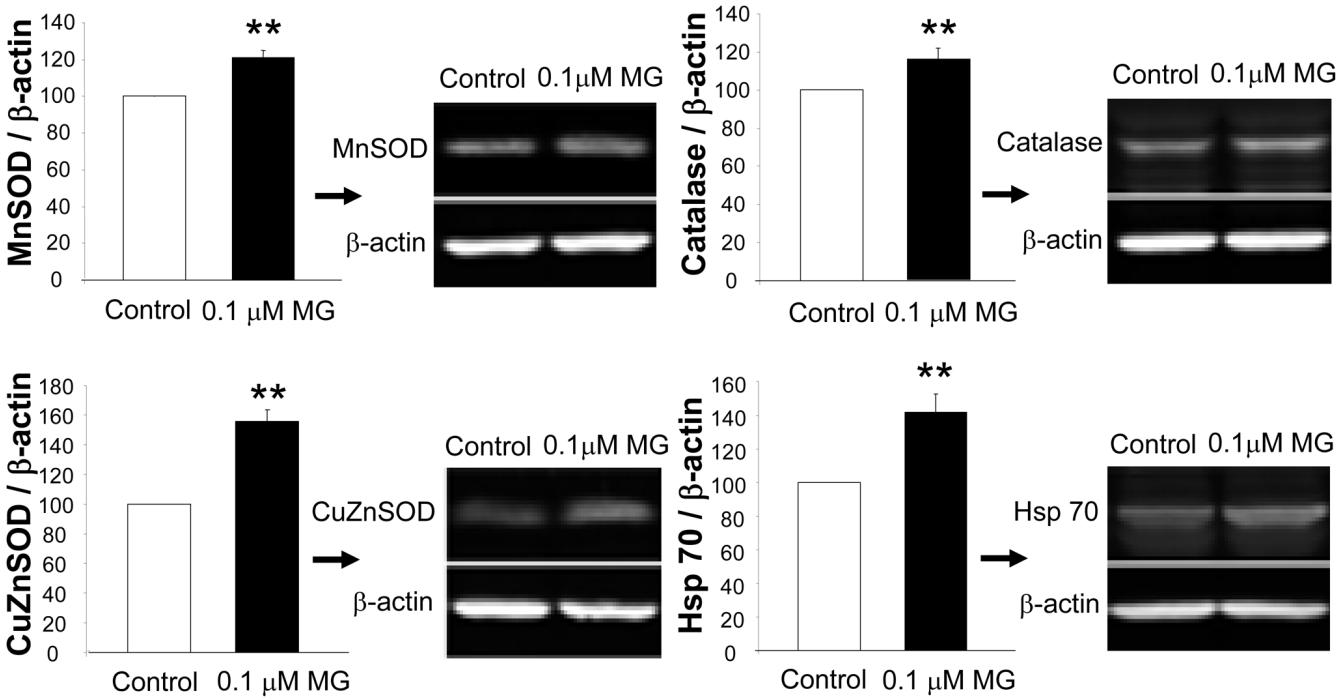

Figure 6. Chronic MG132 was associated with higher protein levels of three antioxidant enzymes and a stress-responsive chaperone

(**A**) Protein levels of SODs, catalase, and inducible Hsp 70 were assessed by Western immunoblotting with infrared secondary probes. β-actin served as a loading control. Data are presented as mean + SEM from 3–7 independent experiments. Two-tailed t test: ***p*<0.05 versus control naïve cells.

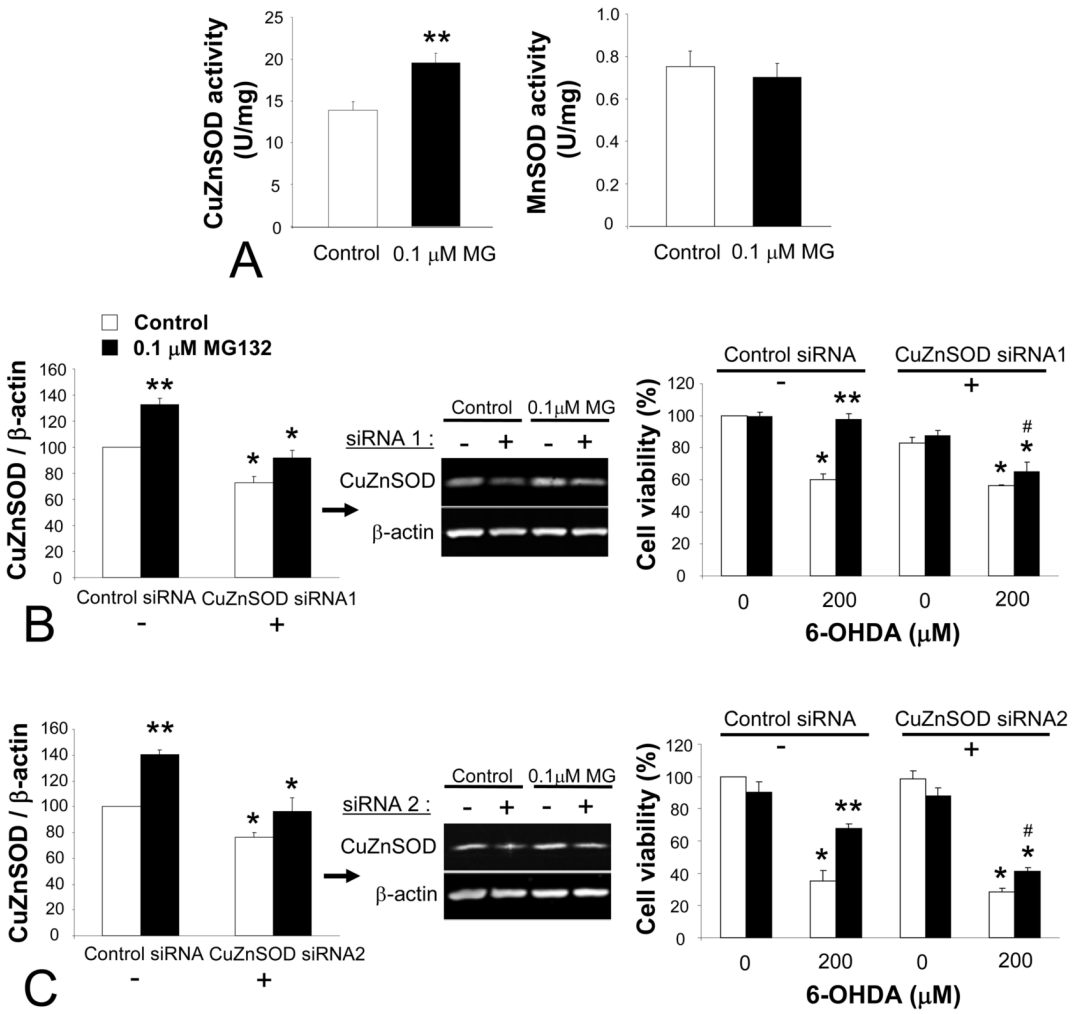

Figure 7. CuZnSOD activity levels are increased with MG132 and CuZnSOD knockdown attenuated protection against oxidative stress

(**A**) SOD enzyme activity assays for CuZn and MnSOD showed an increase in the activity of the former. For SOD activity, 1 Unit is the amount of enzyme needed to exhibit 53% dismutation of the superoxide radical. Two-tailed t-test: **$p<0.05$ versus control naïve cells. (**B** and **C**) On the left are shown quantification of Western immunoblots with negative control siRNA (−) or CuZnSOD siRNA (+) in naïve control (white bars) and chronic MG132-treated cells (black bars). A dose of siRNA that knocked down CuZnSOD levels back to near control values 24 hr later was purposely chosen for these experiments (31 pmoles/cm^2 for both sequences). (**B**) illustrates data with sequence 1 from Qiagen and (**C**) illustrates sequence 2 from Dharmacon. On the right are Cell Titer Glo viability data 24 hr after 6-OHDA treatment. 6-OHDA was applied 24 hr following either CuZnSOD siRNA or the same dose of control siRNA (31 pmoles/cm^2, 88 nM). CuZnSOD siRNA treatment successfully attenuated the MG132-induced rise in viability relative to side-by-side controls. Data are presented as mean + SEM from 3 independent experiments. Bonferroni post-hoc following ANOVA: *$p<0.05$ versus same group with control siRNA in immunoblots on left, and versus same group without 6-OHDA in viability data on right in B and C, **$p<0.05$ versus adjacent white bar of naïve control cells in A–C, # $p<0.05$ versus same group with control siRNA in viability data on the right in B and C.